Contents lists available at ScienceDirect

Journal of Physics and Chemistry of Solids

journal homepage: www.elsevier.com

Characterisation and photocatalytic assessment of TiO_2 nano-polymorphs: Influence of crystallite size and influence of thermal treatment on paint coatings and dye fading kinetics

Norman S. Allen[b, *], Vladimir Vishnyakov[e], Peter J. Kelly[c], Roelf J. Kriek[d], Noredine Mahdjoub[a], Claire Hill[f]

[a] School of Science and the Environment, Faculty of Science and Engineering, Manchester Metropolitan University, Chester Street, Manchester M1 5GD, UK
[b] Institute for Materials Science, University of Huddersfield, Huddersfield, HD1 3DH, UK
[c] Surface Engineering Group, Faculty of Science and Engineering, Manchester Metropolitan University, Chester Street, Manchester M1 5GD, UK
[d] Electrochemistry for Energy & Environment Group, Research Focus Area: Chemical Resource Beneficiation (CRB), North-West University, Private Bag X6001, Potchefstroom, 2520, South Africa
[e] CRECHE, Center for Research in Environmental Coastal Hydrological Engineering, School of Engineering, University of Kwazulu Natal, Durban, South Africa
[f] Cristal Global, PO BOX 26, Grimsby, N.E. Lincs, DN41 8DP, UK

ARTICLE INFO

Keywords:
Nano-particles
Titanium dioxide
Photocatalysis
Anatase
Rutile
Isocyanate-acrylic paint
Crystal size
Temperature treatment
Methyl orange

ABSTRACT

A study on the thermal effects on TiO_2 rutile and anatase nano-powders was undertaken and displayed some unusual photoactivity and crystal structure properties. Rutile nano-particles with different crystallite sizes were characterised and the possible effect on activity were investigated. One of the rutile samples appeared to have trace amounts of anatase and was annealed at high temperatures at 1172 K and 1272 K to highlight the thermodynamic stability phenomenon of titania. Parallel to this study, anatase nano-particles were investigated before and after being annealed up to 1022 K. For all the samples used in this work, characterisation was undertaken using micro-Raman microscopy/XRD and Scanning Electron Microscopy (SEM) while photoactivity assessment was made by measuring and monitoring the photodegradation of a mixture of dye methyl-orange (MeO) and nano-powders under UV-light for 3h30 min in suspension. The study revealed that rutile nano-powder samples were thermodynamically stable even at very high temperatures and poorly active but with an unusual photoactive feature. Concerning the anatase samples; SEM investigation revealed a questioning size growth as the samples showed a different particle size depending on the temperature of thermal treatment. It revealed that annealing at 672 K seemed to be a key temperature as the particles change from a polyhedral structure to a two-dimensional structure showing a platelet like shape. The photocatalytic studies of the anatase nano-particles showed a very high activity especially before annealing. This highlighted the fact that the anatase phase can subsist at high temperatures such as 1022 K and exhibit a persistence in photoactivity even though it has decreased significantly after 672 K. SEM analysis was in accordance with the photoactivity investigation. Nevertheless, the most interesting feature of the results emanates from the reaction order study and rate constant analysis taken from the kinetic shape of the graph of the degradation of MeO as a function of the irradiation time for the different particle sized rutile nanoparticles. Here a zero-order reaction was determined and as a consequence raised questions about the theory of the mechanism of the activities of titania in terms of surface chemistry, surface area dependence and photoactivity. For example, for the nano-rutiles the sample with a 25 nm crystallite size was the most active and the sample with the smallest crystallite size (15 nm) was the least active and yet was found to contain trace levels of nano-anatase. This effect was also substantiated by UV absorption and weathering studies on doped isocyanate-acrylic paint films. UV analysis clearly shows that the absorptivity of the nanoparticles plays a role and correlates with the photoactivity. The 15 nm particles have decreased absorptivity in the near UV and hence decreased activity.

* Corresponding author.
Email addresses: norman_allen@sky.com (N.S. Allen); V.Vishnyakov@hud.ac.uk (V. Vishnyakov); Peter.Kelly@mmu.ac.uk (P.J. Kelly); cobus.kriek@nwu.ac.za (R.J. Kriek); drnlmahdjoub@gmail.com (N. Mahdjoub); Claire.hill@cristal.com (C. Hill)

https://doi.org/10.1016/j.jpcs.2018.11.004
Received 24 October 2018; Received in revised form 9 November 2018; Accepted 11 November 2018
Available online xxx
0022-3697/

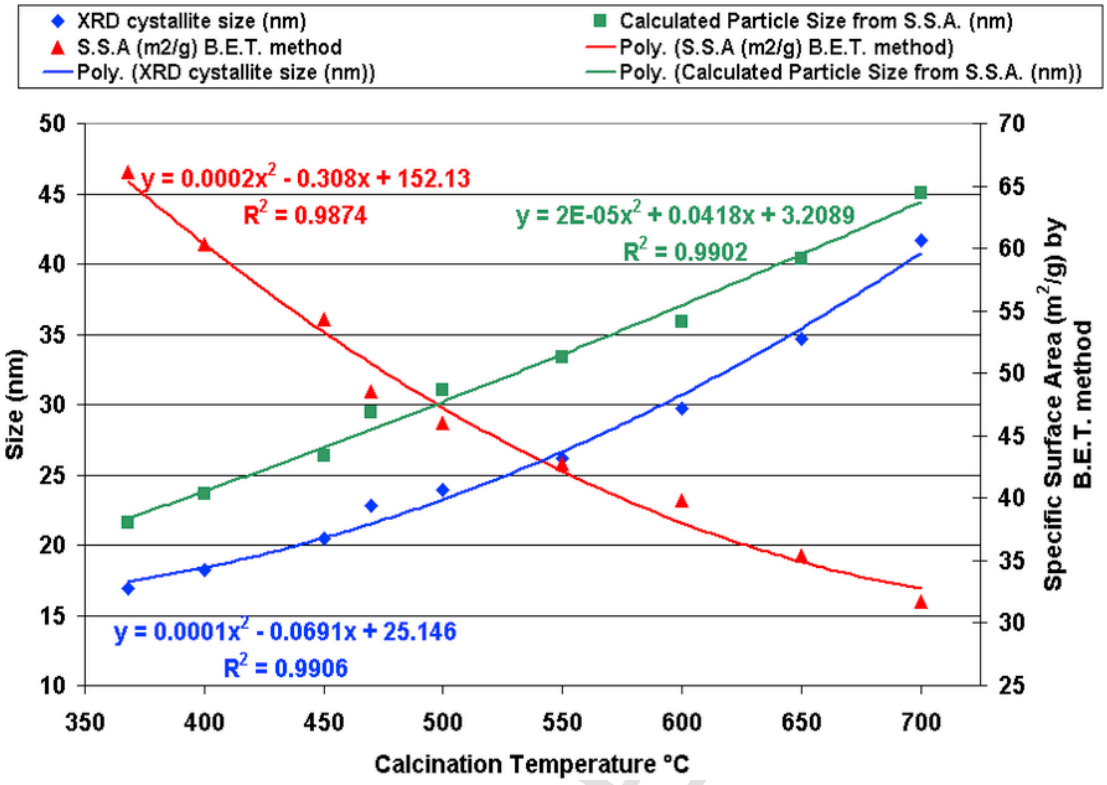

Fig. 1. Calculated particle size from the measured surface area and crystallite size as determined by XRD against calcination temperature.

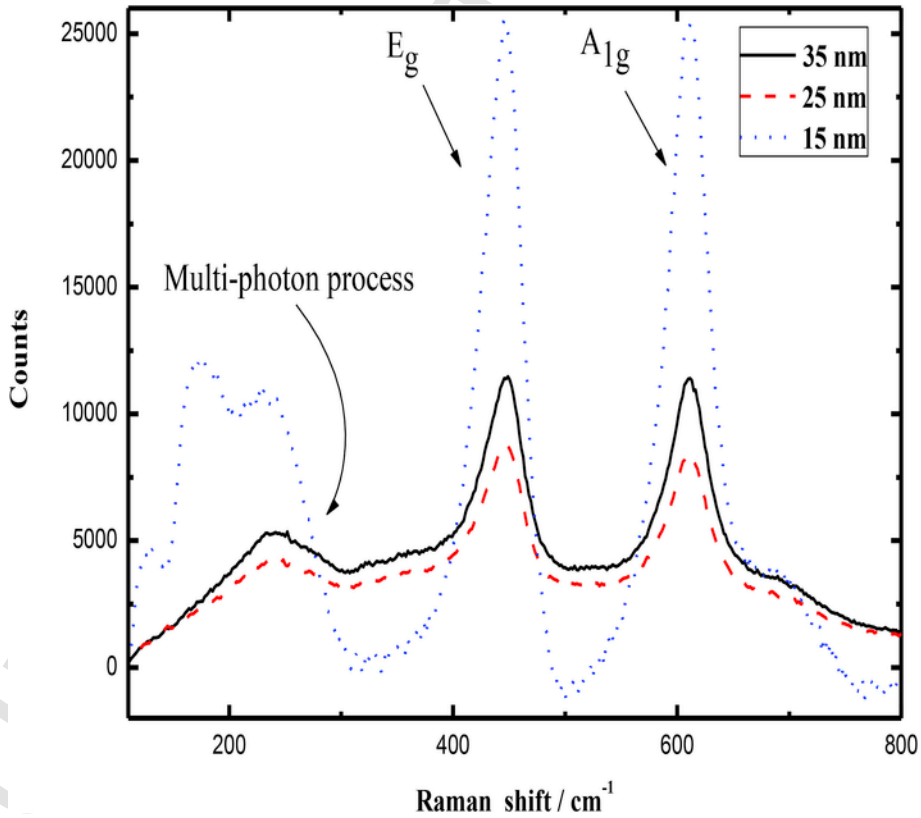

Fig. 2. Raman spectra of the rutile nanoparticles with 15 nm, 25 nm and 35 nm crystallites size.

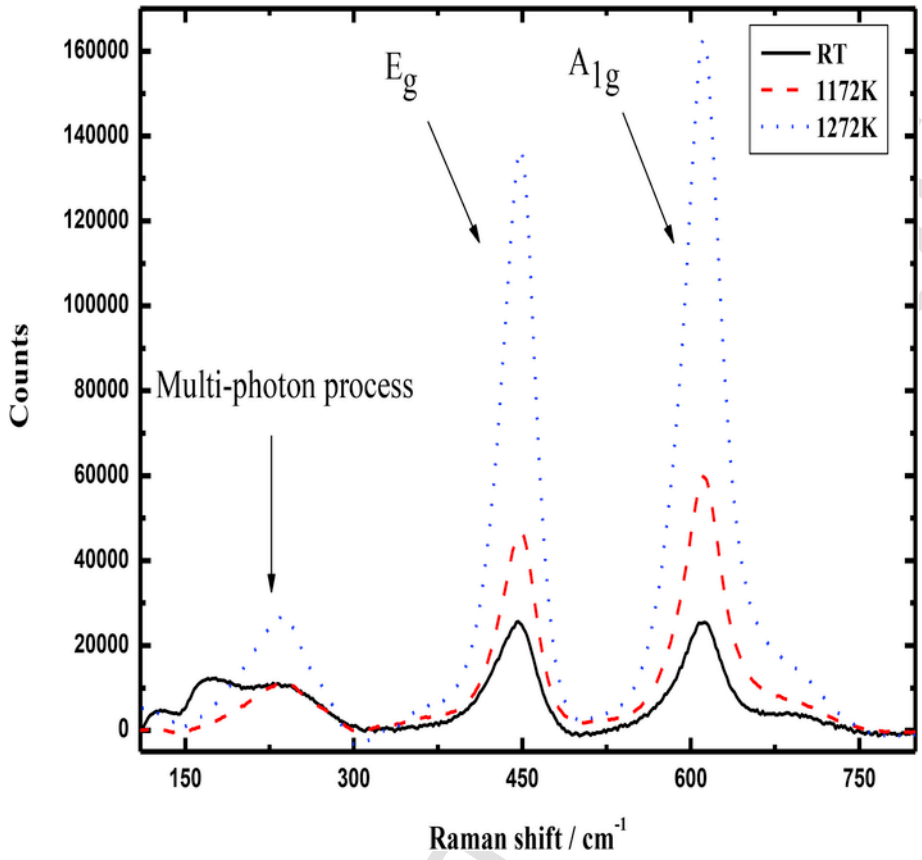

Fig. 3. Raman spectra of the rutile nanoparticle sample with a 15 nm crystallites size annealed at 1172 K and 1272 K.

1. Introduction

Titanium dioxide is a semiconductor oxide with attractive photoactivity properties under UV irradiation [1–3]. The two most studied forms of titania, rutile and anatase, are both photoactive [4–6]. The gap of anatase is equal to 3.23 eV whereas the gap of rutile is equal to 3.02 eV [7]. Anatase is known to be the most photoactive TiO_2 polymorphic material both however, having widespread use as pigments and fillers in polymer materials and coatings. Nevertheless, mixtures of both phases showed particular efficacy, for instance the standard nano-powder P25, from Degussa, is a mixture of 80% anatase and 20% rutile [7,8]. This formulation limits the recombination of charges due to the lower gap of rutile however, their photocatalytic activity depends on the compounds to be degraded; the affinity of anatase in term of adsorption of organic compounds and polymers with the particle surface is one of the most important causes of the degradation activity [9–11]. Many reports have clarified that the photocatalytic activity of TiO_2 strongly depends on its physical properties, surface area, crystallinity and surface acidity to name a few [12–14]. The correlation between the photocatalytic activity and the physical properties of TiO_2 powders, such as crystal structure, surface area, crystallite size and surface hydroxyl groups for example, has been accepted [15–17]. It is believed that the crystal structure is one of the most basic properties used to predict the photocatalytic activity; however, the main property that plays an important role is also well-known to be the surface area and the surface chemistry [18,19]. It has been well accepted that surface area contact is an essential factor for the effectiveness of the catalyst. It is therefore, considered essential to have a nano-powder, in this case, which will have the smallest crystallite size in order to enhance the surface area of contact and therefore the photocatalytic activity [20–

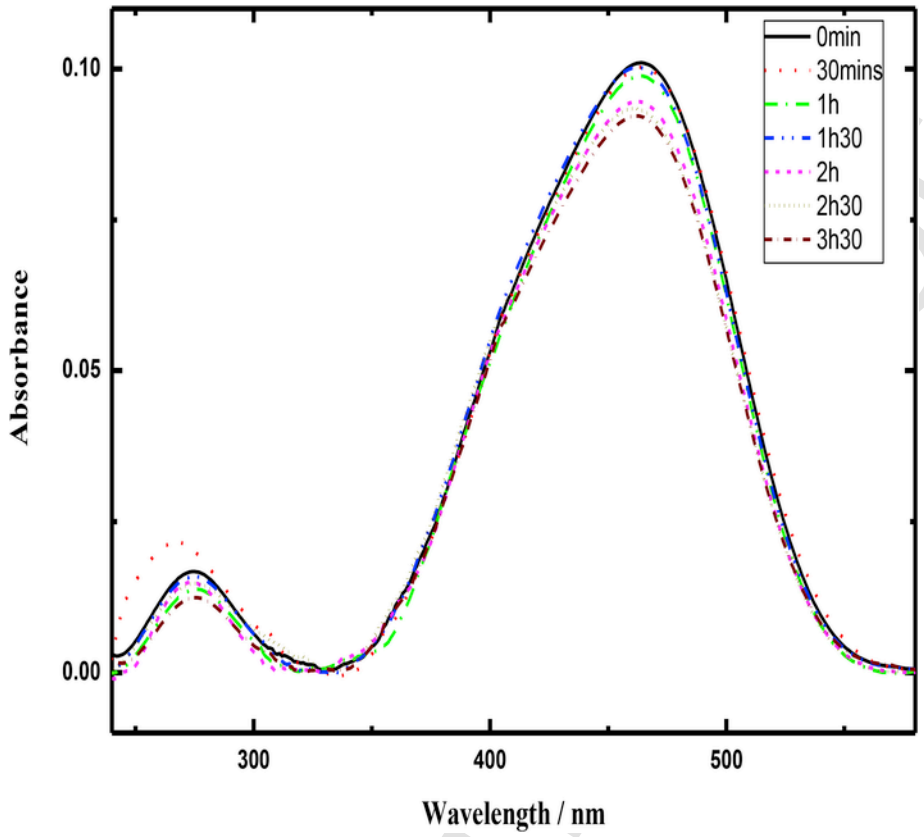

Fig. 4. Example of UV-VIS spectra of the degradation of MeO by the 15 nm rutile sample.

23]. In this work we examine high temperature annealing effects on nano-rutile and nano-anatase particles in terms of their photoactivity. Some novel activity and crystal structure properties are observed and reported showing the anatase polymorph to exhibit high thermodynamic stability. For some nano-rutile particles photoactivity and crystal size has an unusual limitation below 25 nm where photoactivity decreases. This effect is confirmed from both methyl orange dye fading kinetics and solid-state analysis and weathering on doped isocyanate-acrylic paint films.

2. Experimental

2.1. Titania nano-particle preparation

In this work mixed phases of rutile/anatase, pure rutile and anatase have been synthesised. The materials, in nano-particle form were prepared by the common sulphate process route at room temperature. The starting material for the preparation of nanoparticle TiO_2 made here is the "seed" used in the process of manufacturing rutile pigments. Seed can be described as a hydrated titanium dioxide obtained from the thermal hydrolysis of titanium oxysulphate. This TiO2 gel is then digested using concentrated NaOH solution to produce sodium titanate. This is then washed (to remove soluble sulphate and sodium ions) and reacted with either $TiCl_4$ or HCl. This results in a suspension of rutile needles in HCl. The suspension is then neutralised to flocculate the particles; NaOH or NH_4OH can be used at this stage. The particles are then filtered and washed to remove the chloride ions, oven dried and finally calcined to give the desired particle size and specific surface area, which are controlled by calcination temperature and duration (proprietary supplied by CristalGlobal, Grimsby, UK). Commercial samples of rutile as supplied with different crystallites size (15 nm, 25 nm and 35 nm) were characterised by Raman microscopy and were photocatalytically investigated by observing the degradation of methyl orange under UV radiation. One of those samples was annealed at high temperatures up to 1272 K in order to consider the thermodynamic stability of the titania rutile phase. A second batch of commercial titania nanoparticles, consisting of an anatase crystalline structure phase, named PC 105 (CristalGlobal, Grimsby, UK) was annealed at temperatures up to 1022 K and analysed by Raman microscopy and Scanning Electron Microscopy (SEM). Photocatalytic investigations were undertaken by means of the photodegradation rate of methyl orange dye and an isocyanate-acrylic based paint film.

2.2. Material characterisation and testing

The samples were characterised by SEM/XRD and micro-Raman spectroscopy. Micro-Raman measurement was made using an Invia-Microscope from Renishaw. Spectra were taken from each sample in 5–6 places and the results were averaged by running several spectra. The measurements were taken at room temperature with a 514 nm Argon lighter laser. SEM micrographs were taken at room temperature with a Field Emission Gun (FEG) Zeiss Supra 40 VP system.

The specific surface area of the TiO_2 samples were determined using the B.E.T. (Brunauer Emmett Teller) method. The B.E.T. equation can be written in the linear form as follows;

$$P/P_s = 1 + C\text{-}1.\ P$$

$$a(1\text{-}P/P_s)\ a_mC\ a_mC\ Ps$$

Where C is a constant related to the free energy adsorption in the monlayer, p is the pressure of the adsorbate vapour, the amount adsorbed of which is a, P_s is the saturated vapour pressure of the adsorbate at the adsorption temperature and a_m the monolayer capacity of

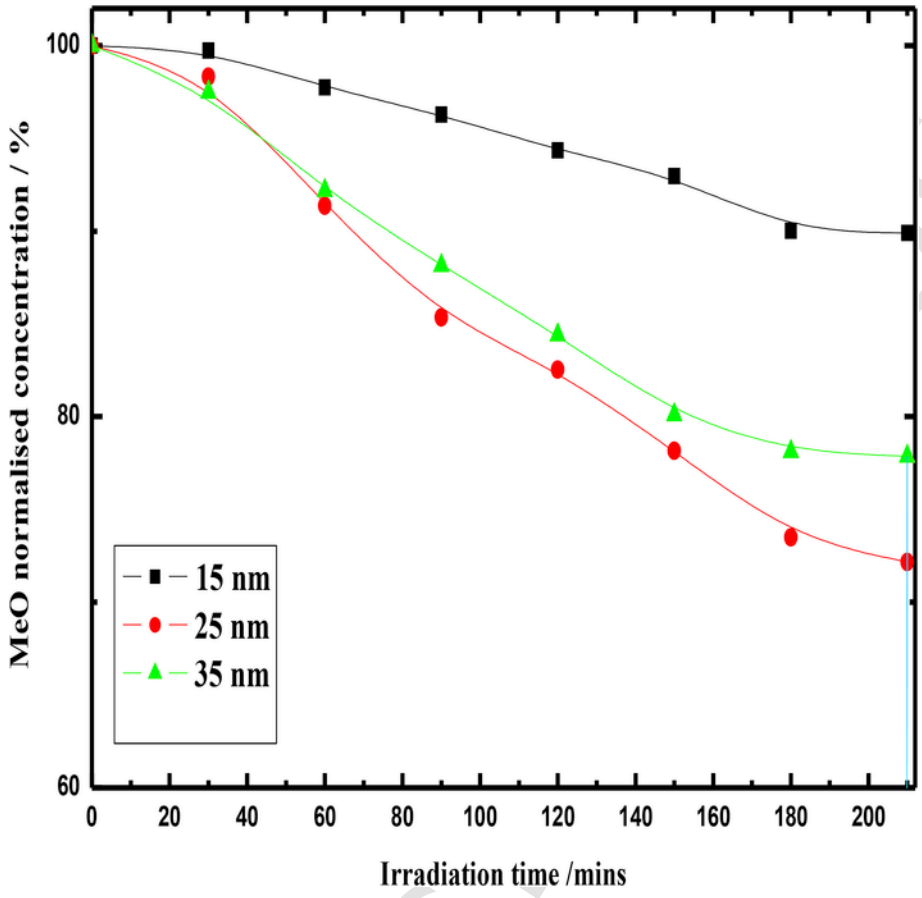

Fig. 5. Reduction of absorption at 472 nm for solutions with the rutile samples with a crystallite size of 15 nm, 25 nm.

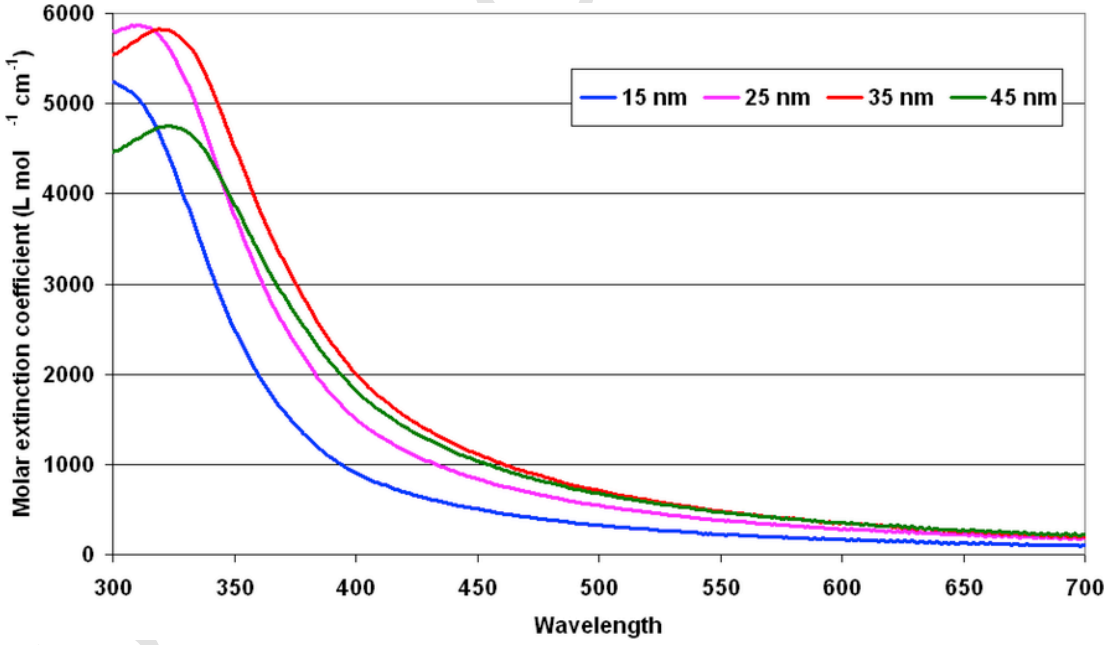

Fig. 6. Molar extinction coefficient plots for TiO_2 of various crystallite sizes. Thin films of isocyanate acrylic containing TiO_2 at 2% on weight of resin solids.

Table 1
Weight loss of an Isocyanate Acrylic Coating Containing Titanium Dioxide of Various Crystallite Sizes (Duplicate Error ± 2mg/100 cm^2).

Hours of Exposure	Crystallite Size (nm)			
	15	25	35	45
200	7.1	4.8	7.2	3.5
400	12	10.1	10.0	6.4
600	19.9	19.0	15.2	12.3
800	29.0	30	22.6	17.5

the surface. In the B.S.I. BET method[170] the adsorption of nitrogen is measured at its boiling point at P/P_s values between 0.05 and 0.3. From the slope and intercept of a plot of the left-hand side equation against P/P_s, values of C and a_m can be evaluated. The value of a_m (in appropriate units) is converted to the specific surface area (usually expressed in $m^2 g^{-1}$) by assuming the molecular area of nitrogen to be 0.1623 nm^2.

The equipment used was a Coulter SA3100. Samples were de-gassed prior to surface area measurement to remove surface adsorbed water which would otherwise interfere with the adsorption of nitrogen during the measurement.

X-ray diffraction is a powerful technique for studying crystal structure. The atomic nuclei in a crystal lattice act as diffraction gratings; the planes of atoms have spacings of a few Angstrom units, which are comparable with the wavelength of x-rays. Scattering of the x-rays by the crystal occurs in certain directions. The primary crystallite size of the nano-sized materials was determined using a Philips PW 1830 diffractometer. Crystallite size was calculated Scherrers equation taking the full width at half maximum (FWHM). The XRD pattern was also used to confirm that the rutile phase had been prepared.

From the line broadening of corresponding X-ray diffraction peaks and using the Scherrer formula the crystallite size was estimated as follows:

$$L = \frac{K\lambda}{\beta \cos \theta}$$

where λ is the wavelength of the X-ray radiation (CuKα = 0.15406 nm), K is a constant taken as 0.89, β is the line width at half maximum height, and θ is the diffracting angle.

The UV/Visible absorption properties of the materials were evaluated using a Perkin Elmer Lambda 20 UV/Vis spectrometer. The light transmitted through a sample compared to a reference is recorded as a function of wavelength. Percentage transmission can then be converted to absorbance (arbitrary units).

For weathering the coated panel samples and plates were exposed in an ATLAS Ci65A accelerated weathering machine. UV irradiance was 0.4 W @ 340 nm and the black panel temperature was 63 °C (50% RH). The test panels were sprayed with water for a period of 12 min in every 120 to simulate the effect of rainfall. Weight loss of the coatings were monitored over the exposure period to assess the coatings durability.

2.3. Reagents and photocatalysis mechanism

The measurements of photocatalytic activity were based on the degradation of the methyl orange (MeO) reagent. Methyl orange (MeO) analytical grade (99.9%) purity from Aesar Alfa was used as a simple model of a series of common azo-dyes. This material is known as an acid-base indicator, orange in basic medium and red in acidic medium. Its structure is characterised by sulphonic acid groups, known to be responsible for the high solubility of these dyes in water.

When it is dissolved in distilled water, the MeO UV-VIS spectrum showed two absorption maxima. The first band is observed at 270 nm and the second, much more intense band is observed at 458 nm. Changes in these reference bands were used to monitor the photocatalytic degradation of MeO by the nanoparticles. Experiments were carried out at room temperature in a static batch photo-reactor consisting of a pyrex cylindrical flask open to air. The use of a magnetic stirrer ensured oxygenation from atmospheric air and a satisfactory mixing of the solution with the nanoparticles. The irradiation of the mixture was performed by using artificial UV–visible halogen light source with an intensity of 0.68 w/m^2 (the instrument used was a "Rank Aldis Tutor 2").

100 cm^3 of the reacting mixture was prepared by adding 0.3 g of TiO_2 particles into distilled water containing some amount (1 cm^3) of MeO (0.06 M). The mixture was stirred and irradiated for 3.5 h; samples of 5 ml were then withdrawn from the reactor every 30 min and separated from the TiO_2 particles using a fine filtering syringe. No sol suspensions were observed in the analysis solution. The MeO removal of the dye solution was determined by measuring the absorbance value at 458 nm, using a UV–visible spectrophotometer calibrated in accordance with the Beer-Lambert's law.

2.4. Preparation of paint films

The isocyanate water based acrylic paint (clear auto-finish) was formulated and supplied by Bayer, Germany. An ambient curing two pack polyurethane clear coating based on isocyanate and acrylic resins was used. Once the paints were prepared, they were drawn-down onto Melinex/cellophane substrates and allowed to dry. The thickness of these films was measured using a gauge. The paints were also applied to stainless steel panels for durability assessment by measuring weight loss upon weathering.

For paint preparation firstly, a millbase containing 30.5% TiO_2 by weight was prepared, the following components were mixed and planetary ball milled with 0.3–0.4 mm zirconium silicate beads for 1 h; 12 g TiO_2, 14.5 g Acrylic resin (Synocure 861X55 manufactured by Cray Valley), 8.6 g butyl acetate (supplied by Samuel Banner & Co Ltd.) and 4.3 g Bannerol G (supplied by Samuel Banner & Co Ltd.). Then 1.46 g of the resulting millbase were added to a let-down consisting of; 26.9 g Synocure 861X55 acrylic resin, 5.0 g butyl acetate, 10.0 g Bannerol G and 0.1 g Fluorad FC430 (manufactured by Fluorchem Ltd.). This mixture was rolled overnight to ensure adequate mixing of the components. Just prior to application of the thin films to the substrates, the second part of the paint, the isocyanate was added, 7.8 g of Desmodur N3390 (manufactured by Bayer). The films were then formed using a spiral wire wound applicator, otherwise known as a draw down bar, onto Melinex (polyester) sheets. Stainless steel panels were also spun coated with the paint for the weathering studies. After application, the solvent was allowed to flash off for a 20 min period, before stoving at 80 °C for 60 min. The dry film thickness on the stainless-steel panels was approximately 25 μm.

3. Results and discussion

3.1. Rutile nanopowders investigation-particle size

Samples of nano-TiO were prepared by the method described in the experimental section. They were calcined at a range of temperatures between 370 and 700 °C for 1 h. The resulting TiO_2 product was ground and then the crystallite size of the primary particles measured by XRD. The specific surface area, using the B.E.T. method was also determined. Fig. 1 demonstrates the effect of calcination temperature on

[1] British standard 4359, Part 1 (1969).

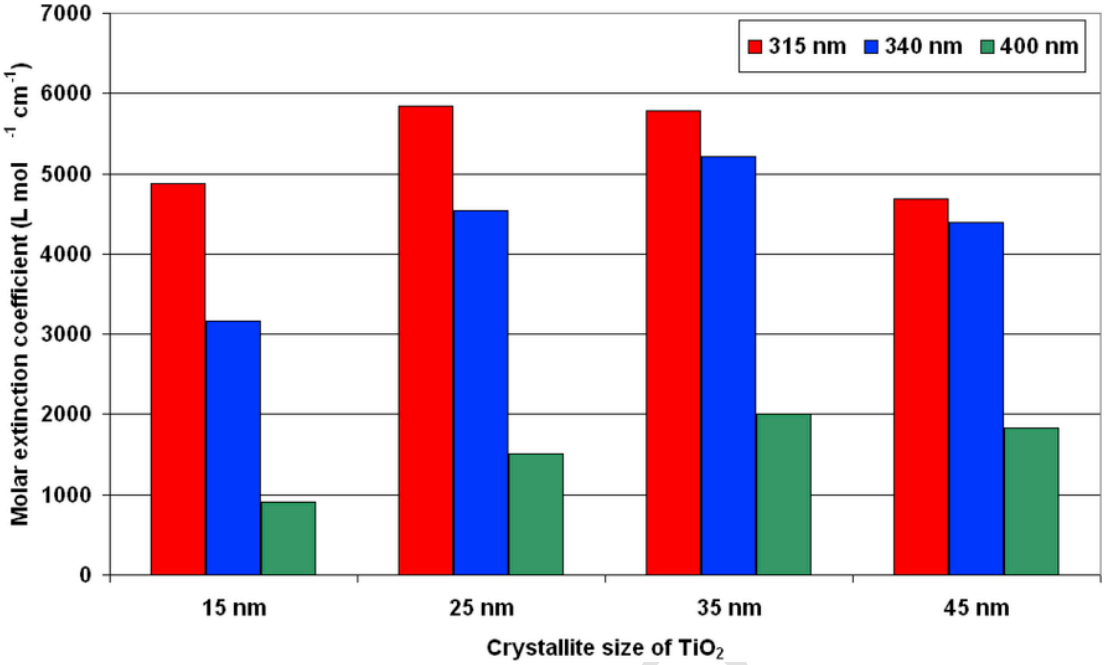

Fig. 7. Molar extinction coefficients for TiO_2 of various crystallite sizes at various wavelengths. Thin films of isocyanate acrylic containing TiO_2 at 2% on weight of resin solids.

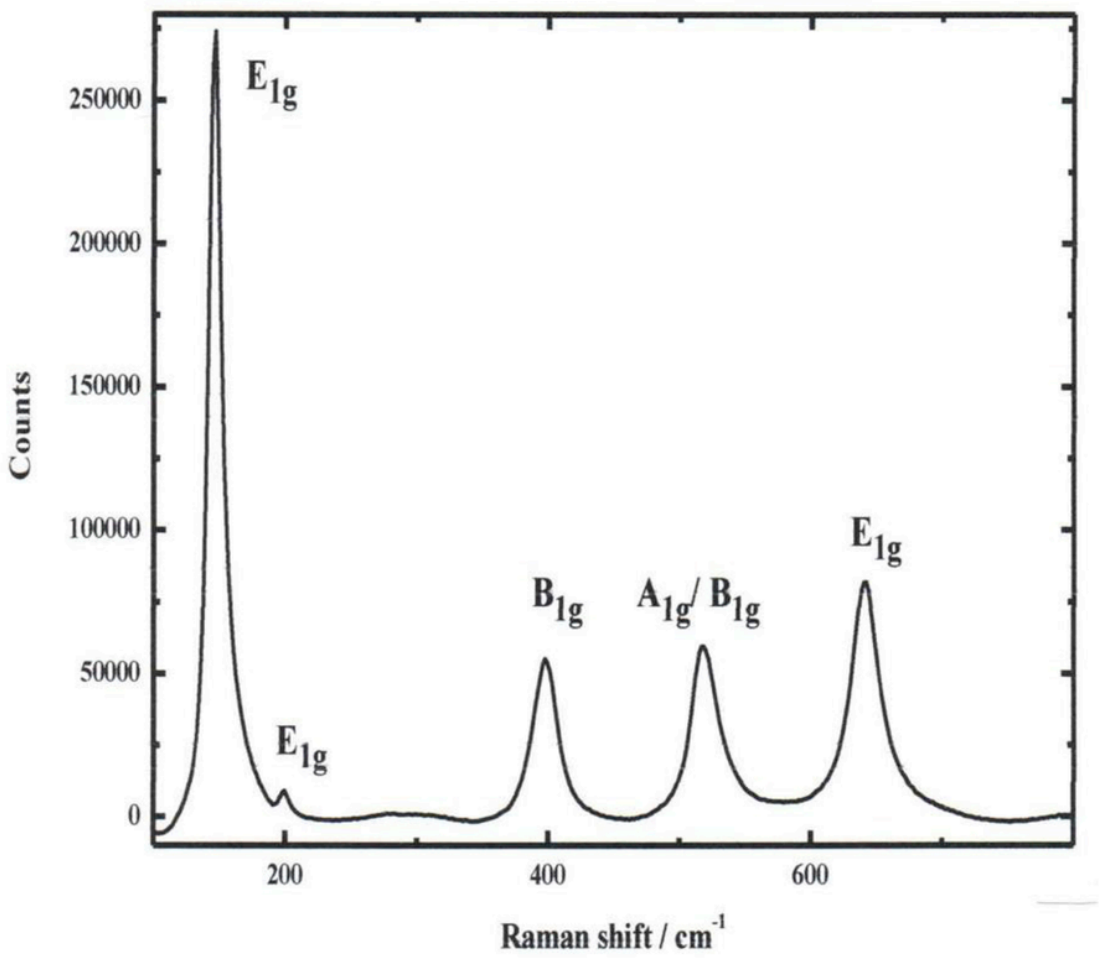

Fig. 8. Raman spectrum of PC 105 anatase nanopowders PC105 as-prepared.

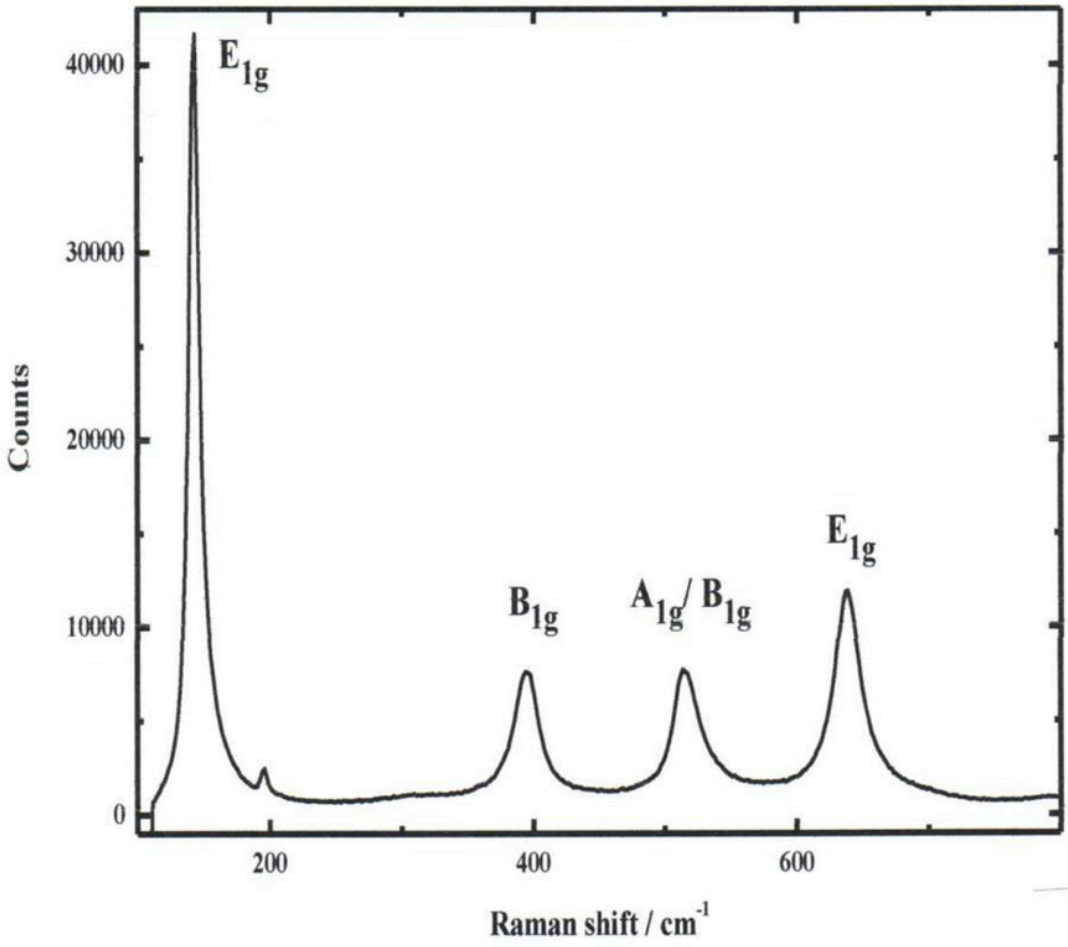

Fig. 9. Raman spectrum of PC 105 anatase nanopowders PC105 at 1022 K.

both of these measured properties. XRD gives the size of the primary crystallites, which in turn agglomerate and increase the particle size as measured, by surface area. From the B.E.T. surface area, the particle size was calculated, the calculation used (Surface Area = (6/(Particle size x density)) assumes that the particles are spherical and have a density of 4.2.

An increase in calcination temperature increases the particle size. Both the size and shape of the TiO_2 manufactured in this way were confirmed by TEM.

3.1.1. Raman study

Rutile nanoparticle samples with different crystallite size were investigated in the first instance. Nanoparticle samples of 15 nm, 25 nm and 35 nm were characterised by Raman microscopy and photocatalytically assessed at room temperature. In order to determine the thermodynamic stability of the rutile TiO_2 form, rutile powders of 15 nm crystallite size were annealed at 1172 K and 1272 K.

The Raman investigation presented by the spectra in Fig. 2 showed the characteristic rutile Raman signature consisting of three peaks, a shoulder at 273 cm^{-1} which is a multi-photon process, the E_g peak at 447 cm^{-1} and the A_{1g} peak at 612 cm^{-1}. The rutile sample at 15 nm crystallite size showed some difference compare to the other samples. Instead of observing an expected shoulder at 273 cm^{-1}, a series of three peaks is visible and are located at 140 cm^{-1}, 195 cm^{-1}, and at 273 cm^{-1}. The peak at 140 cm^{-1} can be attributed to rutile, and is a B_{1g} peak, the peak at 197 cm^{-1} is characteristic of anatase and is usually very weak, and the peak at 273 cm^{-1} is a multi-photon process. As a consequence, the rutile sample with a crystallite size of 15 cm^{-1} was annealed at temperatures up to 1272 K, as shown Fig. 3. The annealing process confirmed the observed thermodynamic stability of rutile, by transforming a mixed rutile-like structure to a pure rutile form with a typical rutile Raman characteristic spectrum. From 1172 K, a rutile phase was identified and subsisted at higher annealing temperatures. A change in the multi-photon absorption raman band at 273 cm^{-1} which is due to a simultaneous absorption of a single photon and emission may supress the photoactivity seen in the 15 nm particles due to enhanced exciton trapping.

3.1.2. Photocatalytic assessment with methyl orange dye

For the purpose of investigating the effect of the size of the rutile crystals on activity, a photocatalytic test was undertaken, and an example of a typical UV-VIS spectrum change is shown Fig. 4. A graph representative of the reduction of MeO concentration is exhibited in Fig. 5. The Titania rutile structure was established as being poorly active. Many studies of course reveal that the titania anatase form is the most active phase. However, since the Raman study revealed the presence of a trace amount of anatase in one of the samples, the rutile sample with a crystallite size of 15 nm, this photocatalytic assessment was in fact essential, since there were new data to consider such as the difference in crystallite size and the trace amount of anatase phase. The results of these experiments certified the poor activity of the titania rutile phase. It is possible to observe, in Fig. 6, the poor activity of the nanoparticles with a different crystallite size. Nevertheless, the order of activity level was not in accordance with the expected theory; here the rutile powder

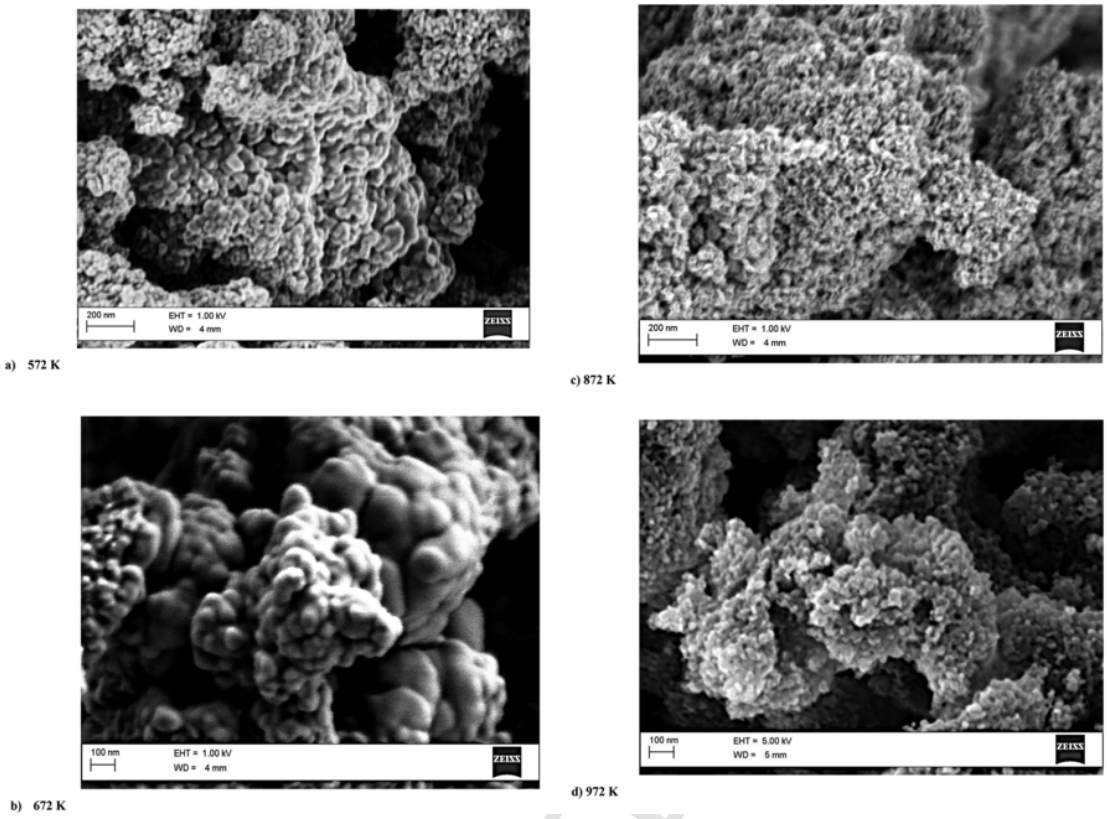

Fig. 10. a-d. SEM micrographs of PC 105 samples at; a)572 K, b)672 K, c)872 K and d)972 K.

activity should follow the order 15 nm > 25 nm > 35 nm. In this case, the rutile nanoparticles with a crystallite size of 15 nm contained a trace amount of the anatase phase. By observing the shape of the graphs illustrating the MeO normalised concentration against the irradiation time (Fig. 6); it is clearly visible that the level of activity of the sample does not follow this expectation and shows that the rutile phase with a crystallite size of 15 nm containing a trace amount of anatase is the least active. In this case, the most active sample was the rutile nano-powder with a crystallite size of 25 nm and the least active was the nanoparticle with a crystallite size of 15 nm with trace amount of anatase. These observations raise important questions about the surface chemistry of titanium dioxide particles, the surface area contact, as the particles with a 15 nm crystallite size should have more surface area and as a consequence be the most active. In this case this well accepted rule is not applicable; another possible theory could be the possible mobility of the free radical electron in the solution as shown in Fig. 5; the reaction follows zero-order kinetics, implying that the concentration of TiO_2 does not play an important role in terms influencing of the activity and therefore, the surface area factor is arguable in this case.

3.1.3. Photocatalytic assessment in isocyanate-acrylic paint film

Measurement of weight loss is a standard analysis procedure in the paint industry for assessing the durability of the coating during weathering under sunlight or simulated sunlight exposure such as in this case the Atlas weatherometer. The data in Table 1 shows that photoactivity of the nanoparticles in the paint film decreases from 25 to 45 nm while that of the 15 nm particles is similar or less active than that of the 25 nm particles. The molar extinction coefficient plots of the dope paint films correlate well illustrating the fact that both the 45 nm and 15 nm doped films exhibit lower absorptivities in the high energy UV end of the spectrum (Fig. 6). The 25 nm doped film has the slight edge in a higher absorptivity in the high energy UV end at 300–315 nm hence its higher activity. This is illustrated by the bar plots shown in Fig. 7 where both the 15 nm and 45 nm doped films exhibit much less absorptivities at 315, 340 and 400 nm. Thus, both the dye fading and paint film weathering correlate well and substantiate each other.

If the particles of TiO_2 are made smaller, they are no longer efficient at scattering visible wavelengths and therefore the amount of light scattered in the visible region decreases. For small particles, at approximately one tenth the wavelength of the scattered light and smaller, Rayleigh [24,25] scattering predominates. The scattering is strongly dependent upon the wavelength of concern where the scattering is inversely proportional to the wavelength to the fourth power. This theory predicts that to scatter UV radiation between 200 and 400 nm, the optimum particle size is between 20 and 40 nm. Smaller particles of TiO_2 will therefore be most effective at scattering radiation with short wavelengths, such as those in the Ultra-Violet (UV) part of the spectrum. Since nano-sized particles of TiO_2 exhibit strong scattering of radiation in the UV part of the spectrum and a minimal amount in the visible, nano-TiO_2 can be used to screen UV. Very small particles may also be more prone to conglomeration hence reducing the surface area contact with the substrate and thus reduced activity but in the solution dye fading the particles were in suspension and less likely to conglomerate.

3.2. TiO_2 anatase nanoparticle investigation-thermal effects

Titania anatase nano-particles were studied as received and were thermally treated at temperatures up to 1022 K.

3.2.1. Raman study

The TiO_2 anatase samples as prepared and calcined at high temperature were characterised by Raman microscopy, examples of the PC 105 type of spectra obtained for all the samples (as received and up to 1022 K) are shown Figs. 8 and 9. The spectra indicate an anatase structure, as expected, with characteristic peaks. The anatase structure, il-

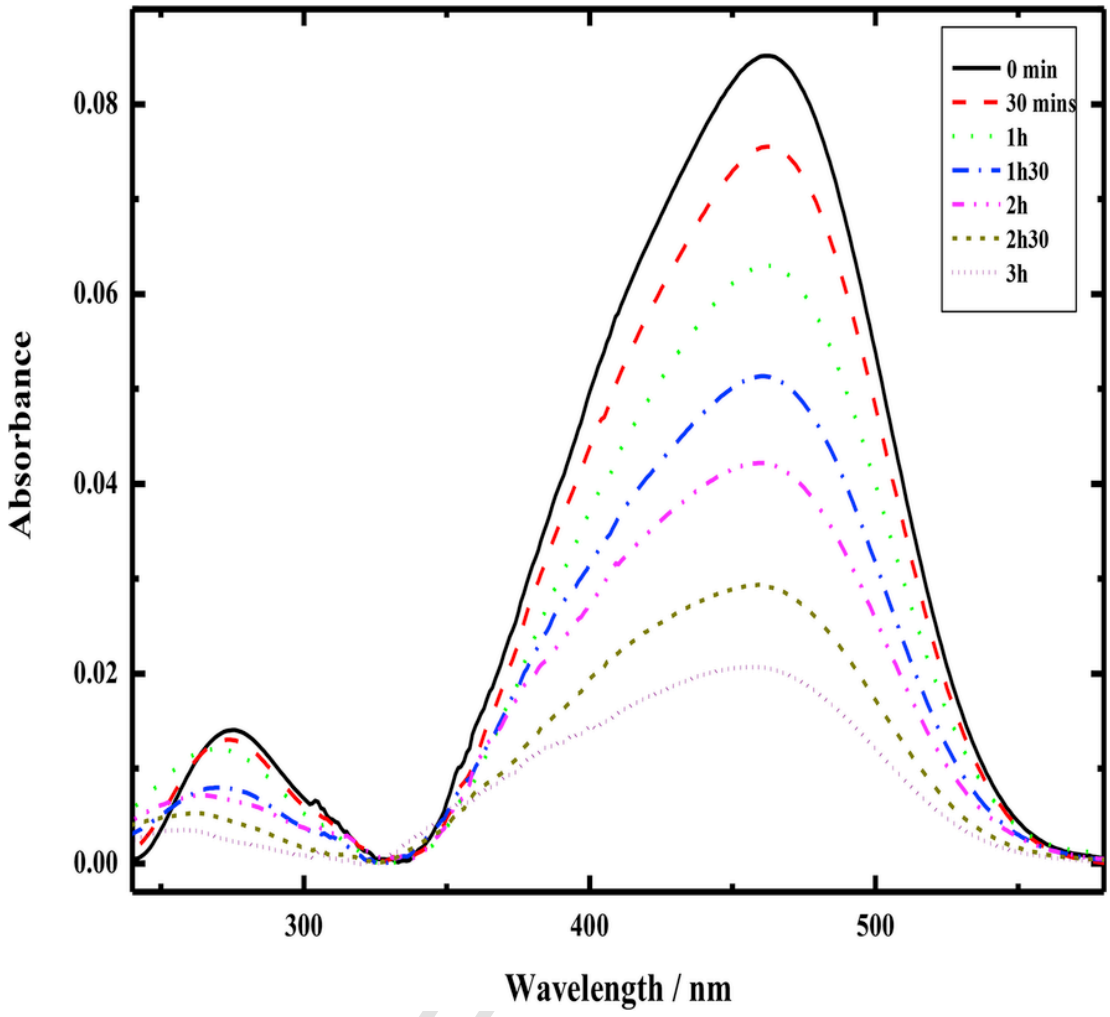

Fig. 11. Example of optical absorption of methyl orange solution after light irradiations with the Titania nano-particles PC 105 sample at 572 K. (For interpretation of the references to colour in this figure legend, the reader is referred to the Web version of this article.)

lustrated in Fig. 9, corresponds to a tetragonal space group. Factor group analysis indicates there are six Raman active modes: $1A_{1g} + 2B_{1g} + 3E_{1g}$. The thermally treated sample also showed a typical anatase phase and no change in structure was observed.

3.2.2. SEM characterisation

Selected SEM images of some of the thermally treated anatase powders are shown Fig. 10; PC105 at 572 K, 672 K, 872 K and 972 K. Detailed image analysis shows that significant parts of particles were polyhedral at 572 K and also appear to be the smallest particles out of the SEM images. The sample annealed at 672 K had the largest particles and had partly melted and formed into aggregates. Interestingly, the logic behind the thermal expansion theory process should have given the samples annealed at the highest temperatures to be the biggest particles, but this is not the case and could be due to the fact that 672 K could be a key-step temperature change in structure. Furthermore, new platelet like structures were visible after calcinations at 872 K for instance and were comparable in terms of crystallite size to the particles treated at 572 K. These SEM data suggests some speculation concerning the fact that initial small crystallite polyhedral grains grow as small particles at temperatures up to 572 K and then change to a platelet like structure above 672 K calcination where they appear melted and much larger. These platelet-like structures were observed with the samples annealed at 872 K and persisted at higher temperatures of thermal treatments up to 972 K.

3.2.3. Photocatalytic assessment

The methyl orange absorption changes are shown in Fig. 11 under degradation by the anatase PC 105 nanoparticles. It is clear, that the intensity of the peaks at 270 nm in the UV region and 480 nm in the visible region decreased progressively according to the time of irradiation as presented.

Fig. 12 shows the normalised MeO concentration (%) as a function of irradiation time at 472 nm for solutions with the samples of nano-particles calcined at different temperatures and characterised by SEM. It shows the high efficacy of the smallest particles to catalyse the decomposition of the MeO dye. The control sample of PC 105 as received had the highest activity compared to the other samples which were thermally treated. Fig. 12 revealed that the samples were active gradually up to 672 K; this observation correlates with the SEM investigation and proves that 672 K is a key temperature for the thermal treatment activation. From about 672 K the nanoparticles changed from a polyhedral structure to a two-dimensional platelet like structure as the activity decreased irregularly up to 1022 K. The photoactivity of the samples annealed at higher temperatures were significantly less active but did not follow the accepted rule of surface area contact relationship to the crystallite size as the sample annealed at 872 K exhibited less activity than the sample annealed at 972 K. Here the platelet like structure is more likely to reduce surface area contact hence reducing activity. A second important observation concerns the shape of the graphs shown

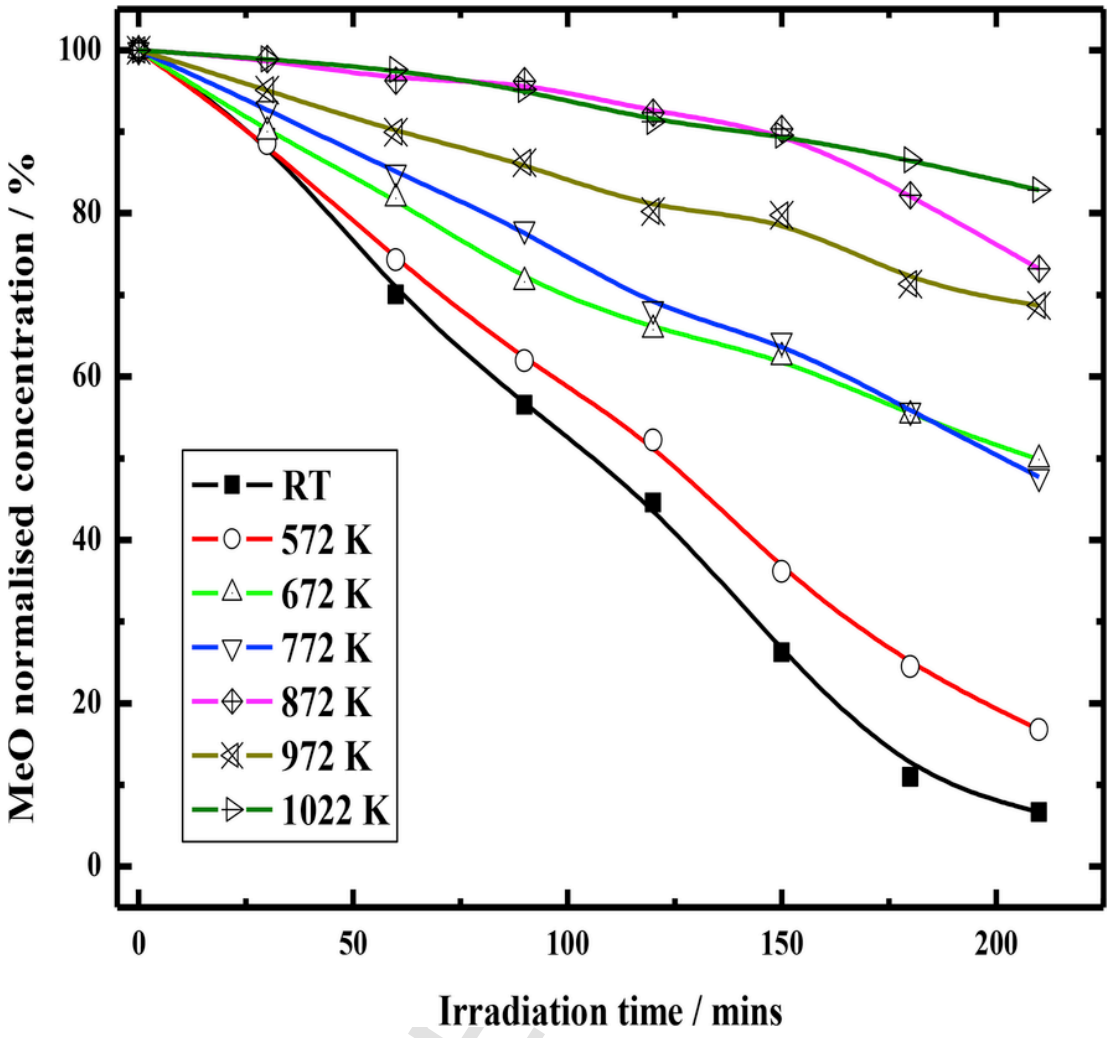

Fig. 12. Reduction of absorption at 472 nm for solutions with PC 105 nano-particles calcinated at different temperatures/K.

in Fig. 12; the shape of these graphs are characteristic of a first order reaction. Fig. 13 illustrates the evolution of the rate constant values according to the temperature of thermal treatment for a first order reaction, the rate constants of the reactions corresponding to each temperature of treatment revealed the importance of thermal treatment and the effect on the reaction as; $k_{RT} > k_{572K} > k_{672K} > k_{772K} > k_{972K} > k_{872K} > k_{1022K}$. Even though all the samples remained in an anatase active phase, the increase in temperature highlighted the fact that the surface was affected by the temperature treatment. In this case, for unheated titania powders Ti^{3+} ions may be formed at the particle/crystal surface due to the release of electrons. In unheated titania the electrons can be stabilised by the hydrated hydroxyl ions on the surface. Heated titania particles will then form $Ti(3^{+})$ ions in the lattice and not on the surface and these may act as recombination centres reducing photoactivity [23]. Thus radicals formed on the surface of unheated titania are assigned to $Ti(^{4+})O(^{\cdot-})Ti(^{4+})OH(^{-})$ species-hydrated. While on heated titania the species are $Ti(^{4+})O(^{2-})Ti(^{4+})O(^{\cdot-})$ [24]. The heating effect clearly resulted in a balance of both species on the titania particle surfaces. The former hydroxylated species were as a consequence the more active ones.

4. Conclusion

TiO_2 rutile and anatase nanoparticle samples were characterised and their photoactivity assessed by monitoring the degradation of MeO dye. Rutile powders with different crystallites sizes (15 nm, 25 nm, and 35 nm) were characterised by Raman microscopy. One of the rutile samples, the one with 15 nm crystallites sizes showed trace amounts of anatase. This sample was then annealed at 1172 K and 1272 K and showed no trace amounts of anatase after thermal treatments. Photocatalytic assessments highlighted the poor activity of the rutile (15 nm, 25 nm, 35 nm) and revealed an unusual level of activity for each sample. The sample with a 25 nm crystallite size was the most photoactive and the sample with the smallest crystallite size (15 nm) was the least active in both the dye fading and isocyanate-acrylic paint film weathering studies. Moreover, the reaction followed a zero-order reaction for the dye study and appeared no to depend on the surface area of the titania particles, opening up some discrepancies on the surface activity chemistry of TiO_2. The reduced absorptivity of the lower activity nanoparticles appeared to account for their reduced photocatalytic activity.

Anatase powder, TiO_2 PC 105 samples, were also characterised as received and annealed at different temperatures up to 1022 K. Raman microscopy investigations showed a characteristic anatase structure persisting after annealing even at very high temperatures. Photocatalytic tests showed the high activity of this sample before and after annealing, PC 105 annealed as received without any thermal treatment showed the highest activity out of all the samples. SEM investigations showed new essential information on the change in structure related to the thermal treatment. Samples annealed up to 672 K remained with a

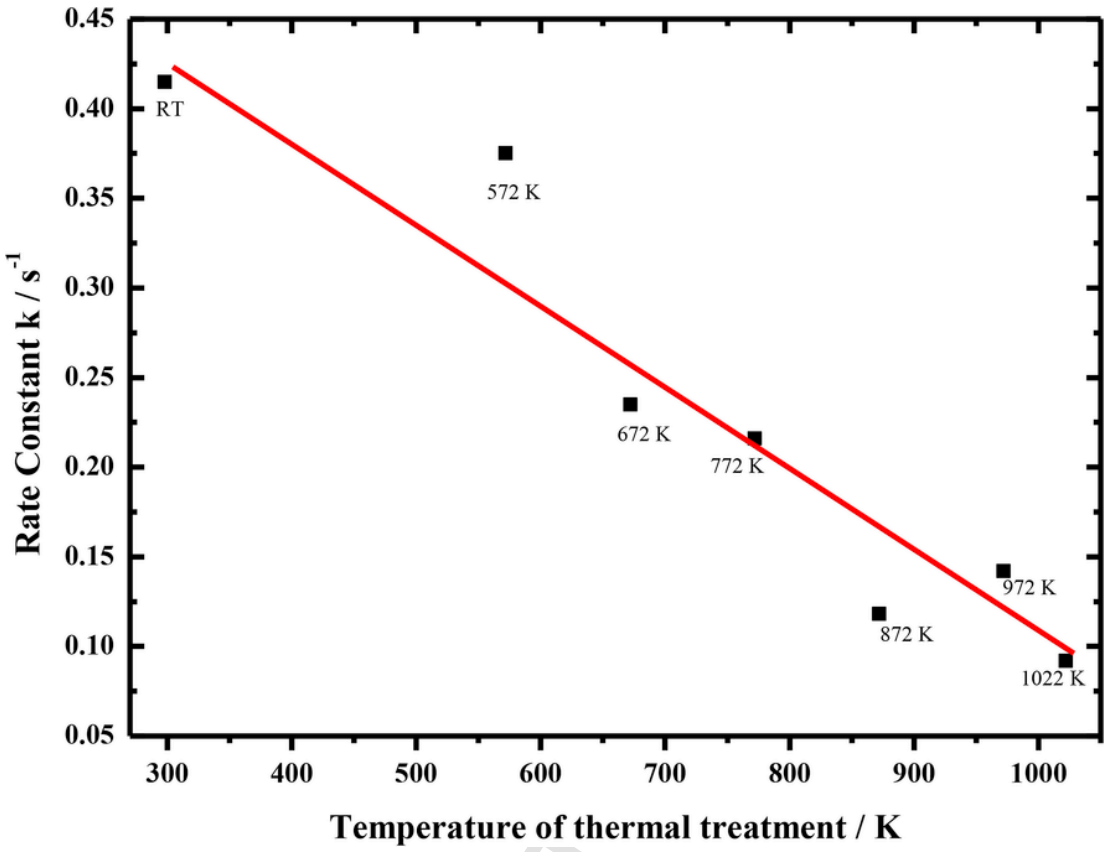

Fig. 13. Temperature of thermal treatment for the PC15/K as a function of the Rate Constant k/s^{-1}.

polyhedral structure, after 672 K the particles changed to a two dimensional like structure; form this analysis 672 K has been identified as key temperature for the change in geometrical structure for TiO_2 nanoparticles in this case. The photoactivity investigation showed that after 672 K this anatase nano-powder appeared not to follow the relationship of surface area/activity [23].

Appendix A. Supplementary data

Supplementary data to this article can be found online at https://doi.org/10.1016/j.jpcs.2018.11.004.

Uncited references

[26].

References

[1] C.H. Ao, S.C. Lee, Combination effect of activated carbon with TiO2 for the photodegradation of binary pollutants at typical indoor air level, J. Photochem. Photobiol. Chem. 161 (2004) 131–140.

[2] Y. Yuac, J.C. Yu, J.G. Yu, Y.C. Kwok, Y.K. Che, J.C. Zhao, L. Ding, W.K. Ge, Po-K. Wong, Enhancement of photocatalytic activity of mesoporous TiO2 by using carbon nanotubes, Appl. Catal. Gen. 289 (2) (2005) 186–196.

[3] M. Inagaki, R. Nonaka, B. Tryba, A.W. Morawski, Dependence of photocatalytic activity of anatase powders on their crystallinity, Chemosphere 64 (3) (2006) 437–445.

[4] Y.N. Masahiro Toyoda, Yuki Nakazawa, M.I. Masanori Hirano, Effect of crystallinity of anatase on photoactivity for methyleneblue decomposition in water, Appl. Catal. B Environ. 49 (2004) 227–232.

[5] H.L. Ma, J.Y. Y, Y. Dai, Y.B. Zhang, B. Lu, G.H. Ma, Raman study of phase transformation of TiO_2 rutile single crystal irradiated by infrared fem to second laser, Appl. Surf. Sci. 253 (2007) 7497–7500.

[6] S.R.-M. Monica Breitman, Alejandro Lopez Gil, Experimental problems in Raman spectroscopy applied to pigment identification in mixtures, Spectrochim. Acta, Part A 68 (2007) 1114–1119.

[7] F. Bosc, A. Ayral, C. Guizard, Mesoporous anatase coatings for coupling membrane separation and photocatalyzed reactions, J. Membr. Sci. 265 (1–2) (2005) 13–19.

[8] H. Park, H.S. Ge, K.H. Chae, J.K. Park, M. Anpo, D.Y. Lee, Improvement of photocatalytic behavior of chemical-vapor-synthesized TiO2 nanopowders by post-heat treatment, Curr. Appl. Phys. 8 (6) (2008) 778–783.

[9] L. Sir ghi, T. A, Y. Hatanaka, Hydrophilicity of TiO2 thin films obtained by radio frequency magnetron sputtering deposition, Thin Solid Films 422 (2002) 55–61.

[10] S. BakardjievaaJan, Š. Václav, Š. Maria, J. Dianezb, M.J. Sayagues, Photoactivity of anatase-rutile TiO2 nanocrystalline mixtures obtained by heat treatment of homogeneously precipitated anatase, Appl. Catal. B Environ. 58 (3–4) (2005) 193–202.

[11] S.J. Seughan Oh, Mater. Sci. Eng. C 26 (2006) 1301–1306.

[12] Q. Ye, P.Y. L, Z.F. Tang, L. Zhai, Hydrophilic properties of nano-TiO_2 thin films deposited by RF magnetron sputtering, Vacuum 81 (2007) 627–631.

[13] L. Peruchon, E. P, A. Girard-Egrot, L. Blum, J.M. Herrmann, C. Guillard, Characterization of self-cleaning glasses using Langmuir-Blodgett technique to control thickness of stearic acid multilayers: importance of spectral emission to define standard test, J. Photochem. Photobiol. Chem. 197 (2–3) (2008) 170–176.

[14] Roland Benedix, F.D., Jana Quaas, Marko Orgass, Application of Titanium Dioxide Photocatalysis to Create Self-cleaning Building Materials. p. 157-168.

[15] S.K. Zheng, T.M. W, G. Xiang, C. Wang, Photocatalytic activity of nanostructured TiO2 thin fims prepared by dc magnetron sputtering method, Vacuum 62 (2001) 361–366.

[16] S. Sakthivel, M.C. H, D.W. Bahnemann, S.U. Geissen, V. Murugesan, A. Vogelpohl, A fine route to tune the photocatalytic activity of TiO2, Appl. Catal. B Environ. 63 (2006) 31–40.

[17] Seong-Soo Honga, M.S. L, Ha-Soo Hwang, S.S. P, Kwon-Taek Lim, Chang-Sik Jua, G.-D. Leea, Preparation of titanium dioxides in the W/C microemulsions and their photocatalytic activity, Sol. Energy Mater. Sol. Cell. 80 (2003) 273–382.

[18] E. Alonso, I. Montequi, M.J. Cocero, Effect of synthesis conditions on photocatalytic activity of TiO2 powders synthesized in supercritical CO2, J. Supercrit. Fluids 49 (2) (2009) 233–238.

[19] C. Bougheloum, A. Messalhi, Photocatalytic degradation of benzene derivatives on TiO2 catalyst, Phys. Procedia 2 (3) (2009) 1055–1058.

[20] Y. Yu, J. Wang, J.F. Parr, Preparation and properties of TiO2/fumed silica composite photocatalytic materials, Procedia Eng. 27 (0) (2012) 448–456.

[21] W. WangJiaguo, Y. Quanjun, X.B. Cheng, Enhanced photocatalytic activity of hierarchical macro/mesoporous TiO2-graphene composites for photodegradation of acetone in air, Appl. Catal. B Environ. 109 (2012) 119–120.

[22] C. Shifu, C. Gengyu, The effect of different preparation conditions on the photocatalytic activity of TiO2·SiO2/beads, Surf. Coating. Technol. 200 (11) (2006) 3637–3643.

[23] A. Fujishima, T.N. Rao, D.A. Tryk, Titanium dioxide photocatalysis, J. Photochem. Photobiol. Chem. Revs. 1 (2000) 1–21.

[24] F. Azeez, E. Al-Hetlani, M. Arafa, Y. Abdelmonem, A.B. Nazeer, M.O. Amin, M. Madkour, The effect of surface charge on photocatalytic degradation of methylene blue dye using chargeable titania nanoparticles, NCBI, Sci. Rep. 8 (2018) 7104.
[25] Craig F. Bohren, Donald R. Huffman, Absorption and Scattering of Light by Small Particles, A Wiley Interscience publication. John Wiley & sons, 1983.
[26] K. Schulte, Application of Micronized Titanium Dioxide as Inorganic UV-absorber, In: 11th Asia Pacific Coatings Conference, 26-27th, June 2001, Bangkok.